Copy 550

CONFIDENTIAL

NASA TM X-60

TECHNICAL MEMORANDUM
X - 60

FLIGHT INVESTIGATION AT SUPERSONIC MACH NUMBERS OF A TORQUE PLUS POSITION SERVOCONTROL SYSTEM

By Clarence A. Robins, Jr.

Langley Research Center
Langley Field, Va.

CLASSIFICATION CHANGED
UNCLASSIFIED
TO NASA TM X-60 11-25-70

FACILITY FORM 602
N71-70829 (ACCESSION NUMBER)
40 (PAGES)
(NASA CR OR TMX OR AD NUMBER)
(THRU)
(CODE)
(CATEGORY)

NATIONAL AERONAUTICS AND SPACE ADMINISTRATION
WASHINGTON
October 1959

CONFIDENTIAL

DECLASSIFIED

1Z

CONFIDENTIAL

NATIONAL AERONAUTICS AND SPACE ADMINISTRATION

TECHNICAL MEMORANDUM X-60

FLIGHT INVESTIGATION AT SUPERSONIC MACH NUMBERS OF A TORQUE PLUS POSITION SERVOCONTROL SYSTEM*

By Clarence A. Robins, Jr.

L
4
5
6

SUMMARY

Flight-test results of a torque plus position servocontrol system in a modified Nike-Ajax missile are presented. Primary consideration of the flight test was minimization of Mach number and altitude effects on the static and dynamic response characteristics of a missile—control-system combination. The flight investigation covered a range of Mach numbers from 1.18 to 2.63 and altitudes from 14,700 feet to 67,600 feet.

The torque plus position servocontrol system employed a torque servo as a hinge-moment-producing control-surface actuator together with carefully chosen amounts of control-surface-position feedback as an input to the torque servo to minimize the effect of variation in flight conditions on missile pitch response and turning rate.

Flight responses of the missile—control-system combination to unit input commands indicated that control-system operation was satisfactory in that both static and dynamic responses of the combination compared favorably with predicted preflight simulator results. Although steady-state responses obtained in flight tests were in fairly good agreement with predicted analytical data, response times of the dynamic responses were slower than expected or considered to be required. The generally well-damped responses at all altitudes in flight are mainly attributed to the conservative system operation indicated as necessary for stability by the preflight simulator used. It is believed that a considerable improvement in response time could be attained; however, a more refined physical simulation of the aerodynamic hinge moments would have been required to show this effect.

*Title, Unclassified.

CONFIDENTIAL

INTRODUCTION

A previous analytical investigation reported in reference 1 showed that a torque-servo-controlled missile utilizing carefully chosen amounts of control-surface-position feedback had favorable static and dynamic response characteristics as compared with a similar missile configuration actuated by a control-surface-position servo. The control-surface-position feedback loop used with the torque servo exhibited a strong stabilizing influence on the damping of the airframe mode. Careful adjustment of the torque servo and control-surface-position feedback gains are shown to have resulted in a minimization of the variation of available missile turning rate due to change in Mach number and altitude. The control system and method of application proposed in reference 1 were flight tested in a two-stage rocket-powered missile, and the results are presented in this paper. Flight-test results obtained were compared with predicted analytical results and with preflight simulator results which directly involved control-system components.

L 456

The torque-servo principle of producing a hinge moment on the control surfaces proportional to a given input signal, which results in a control-surface deflection proportional to the opposing aerodynamic moment, is not new. A recent application of the torque servo is in the control system of a current air-to-air missile.

The airframe in which the torque plus position servocontrol system was flight tested was a slightly modified version of the Nike-Ajax missile (hereinafter usually referred to as Nike), which was used because it was an airframe with known characteristics and also was readily available. Information for determination of stability derivatives of the Nike airframe was obtained from the wind-tunnel data of reference 2, and operational information on Nike control-system components used was taken from reference 3.

SYMBOLS

a_n normal acceleration (referred to center of gravity), g units

$\bar{c}$ mean aerodynamic chord, ft

D linear differential operator, d/dt, sec^{-1}

G control-system static gain, $\left(\frac{\dot{\gamma}}{r}\right)_{ss}$, $\frac{\text{radians/sec}}{\text{r units}}$

DECLASSIFIED

$\frac{\Delta G}{G}$ percentage variation of control-system static gain

H aerodynamic hinge moment acting on control surface, ft-lb

$H_\alpha = \frac{\partial H}{\partial \alpha}$, ft-lb/radian

$H_\delta = \frac{\partial H}{\partial \delta}$, ft-lb/radian

$H_{\dot{\delta}} = \frac{\partial H}{\partial \dot{\delta}}$, $\frac{\text{ft-lb/radian}}{\text{sec}}$

h altitude, ft

I_R moment of inertia of control surface, slug-ft^2

I_X moment of inertia of missile in roll, slug-ft^2

I_Y moment of inertia of missile in pitch, slug-ft^2

I_Z moment of inertia of missile in yaw, slug-ft^2

K_A airframe longitudinal transfer-function coefficient, sec^{-3}

K_T torque-servo static-gain constant, ft-lb/r units

K_α proportionality constant between rate of change of flight path and angle of attack, sec

K_δ control-surface-position feedback proportionality constant, r units/radian

M Mach number

q dynamic pressure, lb/sq ft

r control-surface-actuator reference input signal (in flight tests, the r unit is equivalent to 1.4 volts)

S total wing area in one plane, sq ft

L 4 5 6

CONFIDENTIAL

T	torque-servo hinge moment acting upon control surface, ft-lb
t	time, sec
V	model velocity, ft/sec
α	angle of attack, deg
γ	flight-path angle, deg
δ	control-surface angular deflection (positive when trailing edge is down), deg
ζ	quadratic damping ratio of airframe, nondimensionalized constant
θ	pitch angle, deg
τ	torque-servo transfer-function time constant, sec
τ_D	lag time constant in control-surface-position feedback lead-lag network, sec
τ_N	lead time constant in control-surface-position feedback lead-lag network, sec
τ_s	forward-loop lag-network time constant, sec
ω_n	undamped natural frequency of airframe, radians/sec
C_L	lift coefficient, $\frac{\text{Lift}}{qS}$
C_m	pitching-moment coefficient, $\frac{\text{Pitching moment}}{qS\bar{c}}$

$$C_{L_\alpha} = \frac{\partial C_L}{\partial \alpha}$$

$$C_{L_\delta} = \frac{\partial C_L}{\partial \delta}$$

$$C_{m_\alpha} = \frac{\partial C_m}{\partial \alpha}$$

$$C_{m_\delta} = \frac{\partial C_m}{\partial \delta}$$

CONFIDENTIAL

L 4 5 6

DECLASSIFIED

CONFIDENTIAL

$$C_{m_{\dot{\alpha}}} = \frac{\partial C_m}{\partial \frac{\dot{\alpha}\bar{c}}{2V}}$$

$$C_{m_{\dot{\theta}}} = \frac{\partial C_m}{\partial \frac{\dot{\theta}\bar{c}}{2V}}$$

Subscripts:

h	altitude variation
M	Mach number variation
ss	steady state

A dot over a symbol denotes a derivative with respect to time.

SYSTEM DESCRIPTION

Block Diagram

A block diagram describing the static and dynamic response characteristics of the missile—control-system combination flight tested was used for analysis purposes in this investigation and is shown in figure 1. This diagram and the transfer functions of the airframe, servo, and their feedback loops are similar to those employed for the same purpose in reference 1, with the exception that compensating networks have been added in the control-system forward loop and control-surface-position feedback loop. The feedback loop around the airframe and control-surface blocks does not represent a physical connection but is an aerodynamic loop necessary for system analysis.

A closed-loop transfer function based on an analysis of the block diagram of figure 1 yielded a steady-state gain relationship between the system output $\dot{\gamma}$ and constant input signal r as follows:

$$\left(\frac{\dot{\gamma}}{r}\right)_{ss} = \frac{K_T}{-K_\alpha H_\alpha + \frac{\omega_n^2}{K_A}\left(K_T K_\delta - H_\delta\right)}$$

The expression $\left(\frac{\dot{\gamma}}{r}\right)_{ss}$ is used in a subsequent section for determining the system static-gain parameters K_T and K_δ which yield near minimum variation of $\left(\frac{\dot{\gamma}}{r}\right)_{ss}$ with changes in flight conditions.

CONFIDENTIAL

CONFIDENTIAL

Torque Servo

The torque-servo part of the torque plus position servocontrol system consisted of a modified Nike (pitch or yaw) amplifier, a hydraulic-pressure control valve, and a Nike steering-system-position servo. The pressure control valve driven by the amplifier produced hydraulic pressure proportional to voltage, and this pressure was then converted to force by the servo. Force from the servo was then applied to the control surfaces by means of a connecting-rod bellcrank mechanism and thereby a moment was produced to balance the aerodynamic hinge moment. Some physical characteristics of the servo and pressure control valve used are shown in table I.

The static gain of the torque servo was chosen so as to be well under the saturation limit imposed by the stall torque characteristics of the Nike servo. Dynamic response required of the torque servo established by results of preliminary analytical studies which are discussed in a subsequent section was set by adjustment of a shaping network within the amplifier driving the pressure control valve.

A measured frequency response of the physical torque servo employed in the flight test, but operating under torque loads simulating hinge moments at three flight conditions, is presented in figure 2. Since it was not possible with the physical system to measure frequency response directly between the output and input of the torque servo, the lag network of the control-system forward loop was included and the response measured between the points indicated on the block diagram shown in figure 2. Dynamics of the physical torque servo can be seen to have been characterized by a simple lag transfer function with a time constant τ_s of 0.2 second. The final time constant employed in the lag network of the control-system forward loop was 1.8 seconds.

An analytical frequency response at the same flight conditions and with the same system parameters as the measured frequency response is shown in figure 3. A comparison of the measured and analytical frequency responses shown in figures 2 and 3 reveals the possibility that the physical system measured may have been more accurately described by a third-order transfer function. The nature of the sinusoidal output obtained in the raw frequency response data indicated the presence of nonlinearities in the torque servo and consequently the effect of these nonlinearities was included in the frequency-response plot of figure 2.

Networks

Passive resistance-capacitance (RC) networks were used for stability compensation in the control-system forward and feedback loops: a lag network in the forward loop and a lead-lag network in the control-surface-position feedback loop. The need for inclusion of the compensating networks

CONFIDENTIAL

L 4 5 6

DECLASSIFIED

in the control system is discussed in a subsequent section. Transfer functions of the networks are shown in the block diagram of figure 1.

Airframe

Some of the more prominent physical characteristics of the Nike-Ajax missile used in this investigation are listed in table II, and a sketch of the configuration is presented in figure 4(a). Components of the Nike were used where necessary for this test or were removed and instrumentation substituted with the result that only the roll control system and the sustainer rocket motor were utilized without major modification. Wind-tunnel data from reference 2 were adjusted by a forward center-of-gravity shift for the purpose of linearizing the pitching-moment curve. Stability derivatives used to obtain the analytical results presented in this paper are given in table III. In order for the Nike longitudinal stability derivatives to be more nearly valid, the control-surface plan form used was scaled to coincide with the corresponding Nike control-surface area.

L 4 5 6

The four Nike steering control surfaces were removed and two canard control surfaces of the plan form shown in figure 4(b) were substituted in the pitch plane. Aerodynamic hinge moments for the plan form used were based on hinge-moment coefficients taken from wind-tunnel measurements at the Ames Research Center.

PREFLIGHT INVESTIGATION

Analytical Studies

Analytical methods employed in the investigation of reference 1 for determining static and dynamic characteristics of the torque plus position servocontrol system were used as a basis for obtaining the preliminary analytical results presented in this paper. In brief, these methods followed this procedure: first, the two static gains K_T and K_δ were varied in order to achieve a minimum of change in the complete-system static gain $\left(\frac{\dot{\gamma}}{r}\right)_{ss}$ when the flight conditions were varied and, then, values of K_T and K_δ which yielded near minimum variation in $\left(\frac{\dot{\gamma}}{r}\right)_{ss}$ were used in an analog-computer study to determine their effect on the dynamic response characteristics of the complete system while torque servo, control surface, and airframe dynamic characteristics were varied. Visual examination of analog-computer results yielded a near optimum control-surface viscous-damping value and a set of compensating network

CONFIDENTIAL

and torque-servo transfer-function time constants. These were checked in the physical control system on the preflight simulator.

Preflight Simulator

Preflight simulator checks of the torque plus position servocontrol system were made for the purpose of adjusting physical system gains so that as nearly as possible, statically and dynamically, performance was equivalent to that obtained in analytical studies.

The simulator (fig. 5) was built for a set of three flight conditions, two extreme conditions and one intermediate condition along the anticipated flight path. Simulator checks were carried out by using the components shown in figure 6 and operating in the following manner. An external potentiometer supplied a voltage proportional to the control-surface angular deflection; this voltage was fed into an analog computer which simulated the airframe dynamics. The computer then produced a voltage representing $\dot{\gamma}$ which, through the gain K_α, was proportional to α. Angle-of-attack voltage was then used to operate a position servo that, by means of a framework and set of springs, applied a torque to the control surfaces. The torque acting on the control surfaces because of deflections within the framework and from motion of the framework due to α simulated the total hinge moments exerted by δ and α, respectively.

L 4 5 6

FLIGHT TEST

Launch Technique

A photograph of the flight-test vehicle and its booster, in firing position on the launcher used, is shown as figure 7. The test vehicle was a modified Nike-Ajax missile utilizing for propulsion the standard liquid-fuel sustainer rocket motor within the fuselage and the usual military solid fuel booster shown assembled with the model in figure 7. The launcher is a mobile Nike launcher modified for use independent of Nike missile system fire-control equipment. Using the Nike launcher required that the model be launched in a roll position 45° counterclockwise (when viewed from rear) from the final orientation desired in the flight test.

The Nike roll position gyro was preset before launch to orient the model in an upright position, that is, canard controls horizontal after the missile separated from the booster.

In order to obtain the desired launch angle, which was somewhat lower than normal for the Nike missile, it was necessary to raise the

CONFIDENTIAL

back end of the launcher 20 inches. The launcher after firing was observed to have moved approximately 1 inch with no resulting adverse effects in firing.

Instrumentation

The model was equipped with a 10-channel telemeter which transmitted continuously measurements of normal and transverse accelerations, angle of attack, canard-control-surface and aileron deflections, pitch and roll velocities, and total pressure with a blip superimposed on it to indicate command inputs.

Calibrated accelerometers located on the model longitudinal axis forward and rearward of the center of gravity, since fuel tanks prohibited a center-of-gravity location, were used to obtain normal transverse accelerations. Angle of attack was measured by a standard NASA angle-of-attack vane, and calibrated rate gyroscopes were used to measure pitch and roll velocities. A standard NASA total-pressure probe located on the side of the nose was used to obtain total pressure. A CW Doppler velocimeter measured model velocity during the initial part of the flight; beyond Doppler range the total pressure together with SCR-584 tracking radar data was used to determine velocity. Rawinsonde data were obtained for temperature and atmospheric-pressure calibration over the trajectory of the model.

Command Program

The model was launched at an angle of approximately 70° from the horizontal. A squib-actuated device was used to delay ignition of the sustainer or second-stage rocket motor until 16.4 seconds after launching, in order to have the trajector well within the limits of the flight conditions considered in the preliminary analysis. Sustainer burning lasted for 21 seconds.

Programed commands producing flight maneuvers were square wave pulses of 1.4 volts magnitude, which repeated in a cycle consisting of a series of two pulses approximately 6.8 and 6.4 seconds in duration. Pulse length was based on a compromise of time required for the system response to reach steady state at the highest altitude expected and the necessity for completing a sufficient number of responses along the flight path to permit evaluation of control-system operation over a wide range of Mach numbers and altitudes. Command signals were started on the ground shortly before launch and monitored until firing. Since maneuvers were not desired during boost and for a short time thereafter, the control surfaces were locked at zero deflection prior to launch and were unlocked by the action of the squibs at 7.5 seconds after firing.

CONFIDENTIAL

RESULTS AND DISCUSSION

Preflight Results

By application of the method used in the design approach of reference 1, the static-gain parameters K_T and K_δ that would yield a near minimum variation of the static gain of the model—control-system combination $\left(\frac{\dot{\gamma}}{r}\right)_{ss}$ were determined graphically for the range of anticipated flight conditions. Near optimum values of K_T and K_δ for a minimum variation of $\Delta G/G$ at Mach numbers from 1.2 to 2.4 and an altitude range from sea level to 60,000 feet were obtained by using the data in figure 8. Upon visual evaluation of figure 8, the value of $K_T K_\delta$ considered to yield the nearest to the minimum variation of $\Delta G/G$ for the range of flight conditions covered was 350 ft-lb/radian. The selection of the product $K_T K_\delta$ served to set the control-surface-position feedback gain K_δ at 3.89 volts/radian, because K_T was previously established by the physical capability of the Nike servo and was 90 ft-lb/volt.

L 4 5 6

Then by using the static gains K_T and K_δ previously specified with the airframe and control-surface characteristics, an analog-computer study was made to determine the resulting dynamic response of the control-system—model combination.

A visual evaluation of the computer-study results yielded a combination of system parameters that produced the most desirable system responses of all flight conditions considered. The responses selected were obtained at four representative flight conditions for an r unit step input and are presented in figure 9. Initial studies revealed that in the vicinity of 60,000 feet a magnitude of $H\dot{\delta}$ too large to be physically practical was required for stabilizing the control-surface mode. A lag network in series with the torque servo was employed to maintain control-surface stability and to reduce the need for $H\dot{\delta}$ to a minimum, but this was accomplished, unfortunately, at the expense of slowing down complete system response - an effect not normally associated with control-surface viscous damping. Addition of a lead network in the control-surface-position feedback loop was found to improve system performance at high altitudes. The responses of figure 9 were for a servo time constant of 0.2 second, a lag-network time constant of 0.75 second, lead-lag-network time constants of 0.25 and 0.1 second, and control-surface viscous damping of 1 ft-lb/radian/sec.

Additional analog-computer studies made to ascertain the effects of control-surface mass unbalance revealed no appreciable effects from this source.

CONFIDENTIAL

DECLASSIFIED

Preflight simulator results for the equivalent of r unit step impulses at three flight conditions are shown in figure 10. Only δ and $\dot{\gamma}$ responses were obtained in the preflight simulation since it was not convenient with the analog computer used to simulate the airframe, to record α directly, or to generate $\dot{\theta}$. The pulses in figure 10 were longer than those eventually used in the flight test to enable positive qualitative evaluation of δ and $\dot{\gamma}$ steady-state responses.

A command input voltage, equivalent to the r unit used in obtaining the analytical results, was determined by an open-loop gain measurement of the torque-servo loop and was found to be 1.4 volts. Because of limitations inherent in the construction of the preflight simulator, it was not possible to obtain the full deflection of the framework for simulation of hinge moment due to α at the 59,200-foot altitude condition; consequently, the input was reduced by one-third, and the results are shown in figure 10(c). For the purpose of approximating δ at this flight condition, the simulation was assumed to be nearly linear and the steady-state response of δ was evaluated on this basis. Because of the difficulties involved in simulating the high-altitude condition, steady-state results were not as close nor was the dynamic response considered as reliable as at the two lower flight conditions. Reduction in accuracy of the preflight simulation at the highest altitude was to some extent expected from the effort of a position servo to steady out under a weak spring load.

The main difference noted between the analytical and preflight simulator results from an examination of figure 10 was in the dynamics of the responses of δ and $\dot{\gamma}$. The superimposed oscillations seen in the altitude responses were apparently due, directly or indirectly, to nonlinearities in the control system and preflight simulator. The magnitude and frequency of these oscillations were such that, relative to the overall system response, they were small and apparently contributed no deterrent effects to system stability when pulses occurred while they were present.

Efforts to apply viscous damping to the control surfaces were abandoned after unfavorable oscillatory-system responses resulted from the use of a viscous damper in the physical control system. Lack of viscous damping did not result in control-surface instability as was indicated in earlier computer studies but did alleviate the oscillatory condition and yield a system response that was more damped than the equivalent analytical result. The reason then for stability of the control-surface mode without viscous damping was apparently due to sliding or coulomb friction within the control system. The apparent stabilizing effect of coulomb friction in the torque servo was fairly well substantiated by analog-computer checks made concurrently with preflight simulation, in which coulomb friction was substituted for control-surface viscous

CONFIDENTIAL

damping. Flattened or squared oscillations detected in the δ responses at the 39,500-foot and 59,200-foot flight conditions of figure 10 are similar to those effects known to be directly attributable to coulomb friction as determined in the aforementioned analog-computer checks. Among other nonlinearities thought to have had some effect on stability of the control system was hysteresis which was measured for relatively small displacements of the torque servo. The effects of hysteresis were also investigated in the concurrent analog-computer checks and were found, on the basis of a comparison with preflight simulator results, not to have a particularly significant destabilizing effect. Finally, in addition to the removal of the control-surface viscous damper, it was necessary to increase the compensating lag-network time constant from 0.75 to 1.8 seconds in order to obtain stable system operation at the 59,200-foot altitude on the preflight simulator. The heavily damped response resulting from this increase was found to be only slightly affected by the dynamics of the network in the control-surface-position feedback loop, even though the time constants were altered from the original analytical values.

L 4 5 6

Other than the obvious effect on response times of the δ and $\dot{\gamma}$ responses caused by the differences in lag-network time constants, agreement between analytical and preflight simulator results was good except at 59,200 feet where the preflight simulator response was more damped.

Flight-Test Results

Steady-state response.- Flight response of the control system to three complete cycles of command inputs was obtained from 53 seconds of available telemetered data. These data, which were representative of the flight-test trajectory as well as flight conditions near which analytical results were based, covered a range of altitudes from 14,700 feet to 67,600 feet and Mach numbers from 1.18 to 2.63.

Although the static and dynamic characteristics of $\dot{\gamma}$ were used as a criterion for evaluation of the missile—control-system combination, it was necessary in this investigation to obtain the characteristics of δ, α, and $\dot{\theta}$ in addition to those of $\dot{\gamma}$ so that operation of the physical system could be checked more accurately and ranges of telemeter instruments could be set. Normal acceleration referred to the model center of gravity was also presented, more for correlation of steady-state flight response with predicted values than for the qualitative evaluation of the dynamics of a_n because a_n was similar dynamically to $\dot{\gamma}$ and α.

From a visual examination of the flight data of figure 11, steady state appears to be established in most responses to correlate flight results with analytical results by considering flight conditions at the end of each pulse. An analysis of steady-state flight responses presented

CONFIDENTIAL

CONFIDENTIAL

in figure 11 and the flight conditions at which they occurred are given in table IV, together with computed steady-state responses for the same flight conditions. The steady-state values of α, δ, $\dot{\gamma}$, and $\dot{\theta}$, from table IV were then plotted in figure 12. The product of Mach number and altitude was chosen as a basis for comparison rather than either of the two individually since it was impossible to separate the effects of altitude and Mach number in the flight results.

In figure 12 it can be seen that, for the range of flight conditions considered, values of $\dot{\gamma}$ obtained in the flight test deviated from the corresponding analytical values by a relatively constant value of 0.4 deg/sec with the exception of the pulse ending at 38,000 feet where the deviation was about 0.6 deg/sec. In general, it can be seen that the variation of $\dot{\gamma}$ with flight conditions agrees very well with analytical results.

Figure 12 shows that values of δ were consistently lower in flight than were the analytical values; in fact, for the δ responses of the first half of the command input cycle (fig. 11(a)), it was difficult to distinguish any net deflection. The deviation of steady-state flight responses of δ from the analytical values although large at the lower altitudes eventually decreased and stayed almost constant at altitudes from 40,000 to 65,000 feet. The magnitude of the steady-state flight values of α seemed to take an opposite trend from that of δ, the flight values being consistently larger than analytical values at all flight conditions. It is interesting to note from an examination of figure 12 that the deviation of the flight values of α, $\dot{\gamma}$, and $\dot{\theta}$ from the predicted values followed closely the dynamic-pressure trend, indicated in table IV, to reach a peak at 38,000 feet.

A comparison of the predicted responses of $\left(\frac{\dot{\gamma}}{r}\right)_{ss}$ or G obtained by using torque plus position and position servocontrol systems with flight results obtained by use of a torque plus position servo is presented in figure 13. The position servo considered in figure 13 is described in reference 1. Inasmuch as one of the features of the torque plus position servocontrol system was to minimize the effects of altitude and Mach number on the static response of the complete system, then an ideal result would be no variation of the quantity with the product of altitude and Mach number. It can be seen in figure 13 that the response of the torque plus position servocontrol system results in approximately a $\pm$5-percent variation about a constant 20-percent deviation. The response of the position servo is seen to vary from an initial deviation similar to that of the torque plus position servo until an altitude and Mach number combination of approximately 73,500 feet is reached, or in the flight test an altitude of 37,200 feet, where it increases rapidly to 72 percent.

CONFIDENTIAL

CONFIDENTIAL

Dynamic response.- Dynamic characteristics of $\dot{\gamma}$, α, and a_n contained the same superimposed airframe natural frequency oscillations prevalent during the first two command input cycles of figure 11 but missing during the last two cycles.

During the first complete cycle (fig. 11(a)), considerably more damping of the model overall response as well as of the superimposed oscillation was evident during the first pulse than was evident during the second pulse; however, in general, damping of the overall response at other flight conditions did not vary greatly from pulse to pulse. Comparison of the dynamics of $\dot{\gamma}$ flight responses with trends of overall damping displayed by preflight simulator responses indicated good agreement. Because of the oscillatory nature and apparent low magnitude of δ during the first two complete cycles of pulses, a comparison with analytical dynamic results was not attempted; however, there was a striking similarity between the δ responses for the final two pulses (fig. 11(c)) and the preflight simulator result at 59,200 feet (fig. 10(c)), especially in the squaring effect common to each response that was attributed mainly to coulomb friction. From an examination of the telemetered time history, it was apparent that roll rate did not exceed 9 deg/sec throughout the part of the flight from which the data presented in this paper was taken.

L 456

Comparison between flight and analytical results.- An examination of all the flight results showed that δ tended to pulse about a position other than zero, which influenced the other flight results in the same manner. This was due probably to one or all of the following reasons:

(1) Drift in the electrical centering of the torque servo

(2) Out-of-trim moment of the airframe

(3) Body bending

The airframe frequency oscillations superimposed on all the flight responses during the first two command cycles and which disappeared during the final high-altitude command cycle were probably due to dynamic-pressure effects associated with airframe disturbances. At 60,000 to 70,000 feet it does not seem that dynamic pressure would have diminished sufficiently for the oscillations to disappear; therefore, other effects were present and among them was believed to be structural damping because of the nature of construction of the airframe. The change in damping of the responses to the first two pulses of figure 11 occurred almost simultaneously with the beginning of the second pulse and the ignition of the sustainer rocket motor. The latter seems to have been responsible for the increased stiffness of the overall system response and reduction of oscillation magnitude.

CONFIDENTIAL

The relatively wide variation of steady-state flight responses of δ and α from predicted values and the reasonably good agreement between those of $\dot{\gamma}$ and a_n indicated that whatever caused the differences in δ and α apparently did not significantly affect $\dot{\gamma}$ and a_n. The reason for this inconsistency of results was believed to be due to body bending, which was a prominent characteristic of the airframe used. Numerous assemblies and disassemblies would seem to make the model even more flexible. The angle-of-attack indicator located at the most distant point possible from the center of gravity was considered most likely to reflect the effects of any body bending if present, which was apparently the case. Static deflection of the order of 1 deg/g in the vicinity of the nose was observed prior to the flight test. First approximation calculations using flight data at the 38,000-foot flight condition based on a first body bending frequency of 20 cps showed that differences between flight and analytical results of 2° or more due to body bending were well within reason. Furthermore, it was noted previously that the difference between flight and analytical values of α was almost directly proportional to dynamic pressure. It seems, however, that any effect, such as body bending so strongly exhibited by α, would be reflected in the δ response of a canard control-forward configuration, such as used in this investigation, and that this effect would be in the form of lower apparent control-surface deflections than were predicted. It was of interest to note that, between the time of launch and control-surface unlocking, the control-surface position changed by -0.8°. Notwithstanding the fact that telemeter frequency could have shifted, there was also the possibility that hinging of the airframe may have occurred since the control-surface-position recorder was in one section of the model and the control-surface lock was in the next rearward section.

L 4 5 6

Although some of the effects due to what was thought to be the more outstanding nonlinearities existing in the control system were determined in preflight simulator checks, there were, obviously, other nonlinearities present which affected the airframe in a manner that defied their isolation and identification.

Hinge-moment data for the control surfaces used in calculating predicted data were based on coefficients obtained in wind-tunnel tests of a model with the control surfaces mounted on a cylindrical body section; whereas, in this investigation the control surfaces were attached to a tapered section of the model. This factor would definitely have reduced the accuracy of the control-surface and aerodynamic feedback transfer functions. Any change in control-surface effectiveness, however, which may have resulted from the fact that wind-tunnel data of the Nike airframe were obtained with a standard set of Nike control surfaces whose configuration was slightly different from the plan form of the control surfaces actually used in the flight test, was ignored in the analytical studies.

The exact inertia of the loaded (fuel) condition of the model was not determined; therefore, an approximation was made, based on Nike data. The empty (fuel) condition inertia was measured and found to be about 9 percent lower than that used in analytical calculations; this difference had the effect of raising both the airframe natural frequency and damping, a condition which favored stability and was a contributing factor toward the increased damping not anticipated at the highest altitudes in the flight test.

The original analytical results were obtained by using a lag-network time constant of 0.75 second and a viscous damper with the control surface; however, since flight results were obtained by using a lag-network time constant of 1.8 seconds and without a viscous damper, it was decided to make a comparison of the two responses for closer observance of nonlinear effects and other contributing factors discussed previously. The results of the post-flight simulation are shown in figure 14. From a comparison of the results of figure 14 and the flight data in figure 11, it is evident that agreement of the first two flight command cycles is good, but at the highest altitude the linear response appears to be much less damped than the flight result. The oscillatory nature of the simulated response at 65,000 feet was known to be caused by addition of coulomb friction in the system; however, in view of the well-damped flight response under the same flight condition as well as the appearance of coulomb friction in the δ response, it would seem that the airframe actually filtered out friction and other nonlinearities which caused oscillations in both the linear and preflight simulation.

L 4 5 6

CONCLUSIONS

A torque plus position servocontrol system has been flight tested in a modified Nike-Ajax missile with the primary concern being the minimization of Mach number and altitude effects on missile static and dynamic response characteristics, especially as related to missile turning rate. Results of the flight test were compared with analytical and preflight simulation data and the following conclusions were reached about the control system tested:

1. Preflight simulator checks indicated that a mechanical viscous damper was not a satisfactory means of control-surface damping but that coulomb friction within the torque plus position servocontrol system seemed to achieve as good or better results than expected from use of a viscous damper.

2. The method employed in simulating physical aerodynamic hinge moments, particularly those due to angle of attack, was considered to

have dictated the use of more stability compensation than was necessary. The additional stability resulted in considerably slower response times than were expected. It is believed that a substantial improvement in response time could be attained; however, a more refined physical simulation of the aerodynamic hinge moments would have been required to show this effect.

3. Effects of body bending noted in flight data were not considered to have substantially affected missile turning rate or damping in pitch, which were the criteria of missile—control-system performance.

4. Flight dynamic responses in general exhibited a higher degree of damping in pitch than those predicted by analytical data.

5. Maneuvers performed in the flight test confirmed satisfactory operation of the torque plus position servocontrol system for unit input commands, and it is believed that the flight test verified a method of minimizing the effects of variation of flight conditions on the static and dynamic characteristics of a missile—control-system combination.

Langley Research Center,
National Aeronautics and Space Administration,
Langley Field, Va., May 26, 1959.

REFERENCES

1. Nason, Martin L.: An Evaluation of an Aeromechanical Method of Minimizing Servo-Missile Transfer-Function Variations With Flight Condition. NACA RM L56A31, 1956.

2. Covey, Robert E.: Test of a 0.075-Scale Model of the Douglas Nike 1249B Missile in the 20-Inch Supersonic Wind Tunnel (Period V). SWT 20-36, Jet Propulsion Lab., C.I.T., Jan. 1954.

3. Anon.: Guided Missile System, XSAM-A-7. Missile and Booster - Missile Guidance Section, GS-16725. Vol. III - Maintenance Notes. Contract DA-30-069-ORD-1295, Bell Telephone Labs., Inc., June 1954.

CONFIDENTIAL

L 4 5 6

TABLE I

TORQUE-SERVO PHYSICAL CHARACTERISTICS

Nike-Ajax servo:	
Length of piston stroke, in.	1.204
Effective working area of piston, $in.^2$	0.441
Maximum stall torque, in-lb	1.365
Pressure control servo valve (Cadillac PC2):	
Supply pressure, psi	500 to 3,000
Sensitivity, psi/ma differential current	375
Internal leakage (3,000 psi supply pressure; 90° F), gal/min	0.25

CONFIDENTIAL

L
4
5
6

TABLE II

MODIFIED NIKE-AJAX MISSILE PHYSICAL CHARACTERISTICS

I_X (less sustainer fuel), slug-ft^2	5.79
I_Y (less sustainer fuel), slug-ft^2	745
I_Z (less sustainer fuel), slug-ft^2	745
Weight, lb	840
Sustainer fuel, lb	310
Sustainer rate of burning (approx.), lb/sec	14.75
Overall length, in.	251
Fuselage diameter (not including tunnels), in.	12
Total wing area in one plane, sq ft	17.54
$\bar{c}$, ft	5.4
Center-of-gravity location (from zero station), in.	136

CONFIDENTIAL

TABLE III

STABILITY DERIVATIVES[1]

Mach number	C_{L_α}	C_{m_α}	C_{m_δ}	C_{L_δ}	$C_{m_{\dot{\theta}}}$	$C_{m_{\dot{\alpha}}}$
1.2	1.98	-0.225	0.216	0	-2.52	0
1.6	1.87	-0.210	0.199	0	-2.37	0
2.0	1.77	-0.194	0.183	0	-2.16	0
2.4	1.67	-0.177	0.168	0	-1.92	0

[1]All derivatives are in per radian measure and are based on $S = 17.54$ square feet, $\bar{c} = 5.4$ feet, and a center-of-gravity location at station 136.

CONFIDENTIAL

TABLE IV

COMPARISON OF STEADY-STATE FLIGHT AND ANALYTICAL RESULTS

	Mach number, M	h, ft	V, ft/sec	q, lb/sq ft	δ, deg	$\dot{\gamma}$, deg/sec	α, deg	$\dot{\theta}$, deg/sec	a_n, g units
Flight	1.24	22,500	1,313	986	-0.2	2.25	4.0	2.5	1.95
Analytical					2.67	1.87	2.5	1.87	1.33
Flight	1.56	29,500	1,600	1,171	-0.8	2.25	4	2.5	1.65
Analytical					2.6	1.85	2.44	1.84	1.6
Flight	2.02	38,000	1,975	1,330	1.5	2.4	5.0	3.0	2.4
Analytical					2.69	1.82	2.52	1.83	1.95
Flight	1.854	65,000	1,782	291	5.5	1.75	8.5	2.0	1.8
Analytical					7.22	1.35	6.8	1.35	1.3

CONFIDENTIAL

CONFIDENTIAL

CONFIDENTIAL

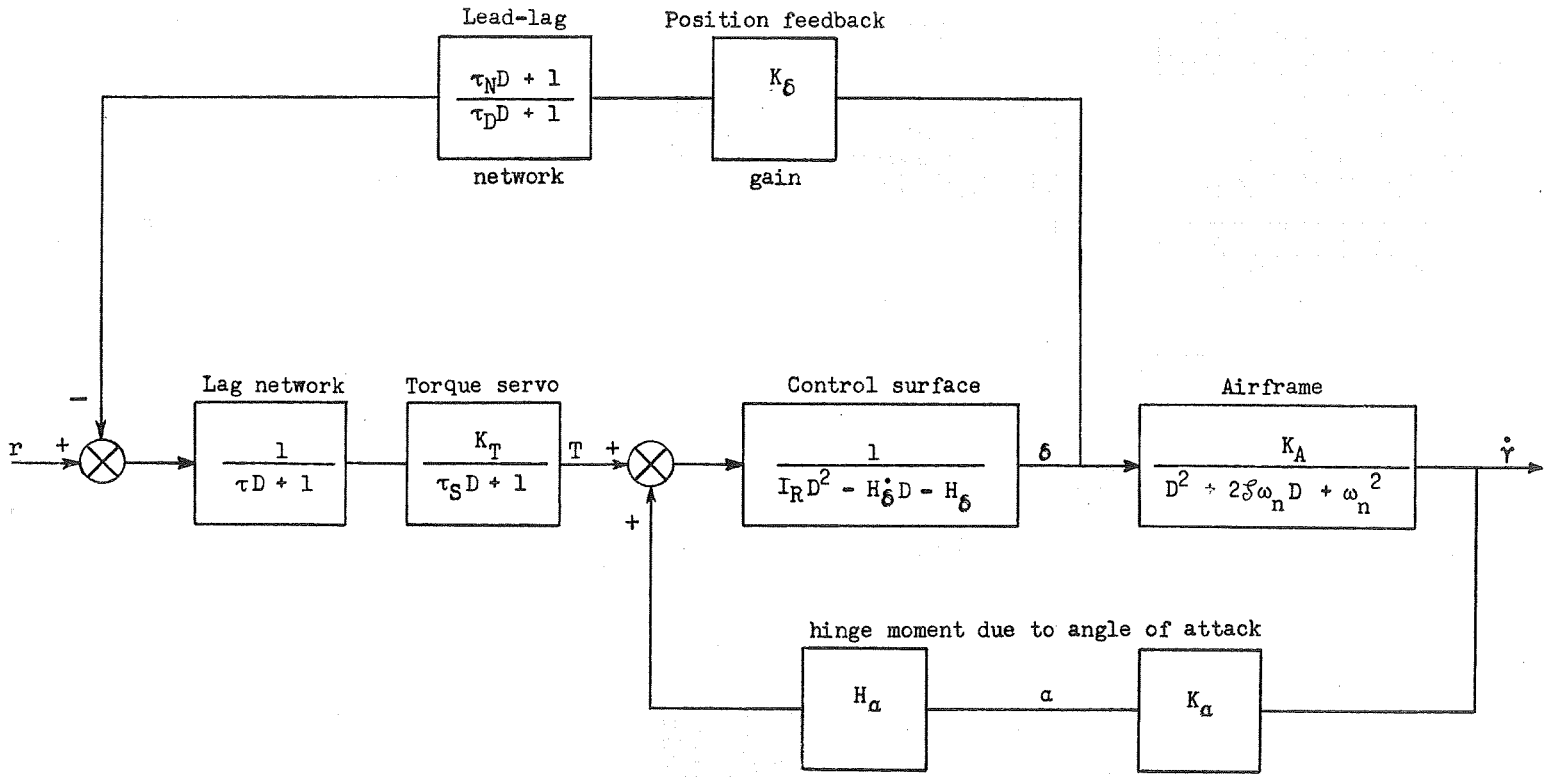

Figure 1.- Block diagram of a modified Nike-Ajax missile airframe actuated by a torque plus position servocontrol system.

L-456

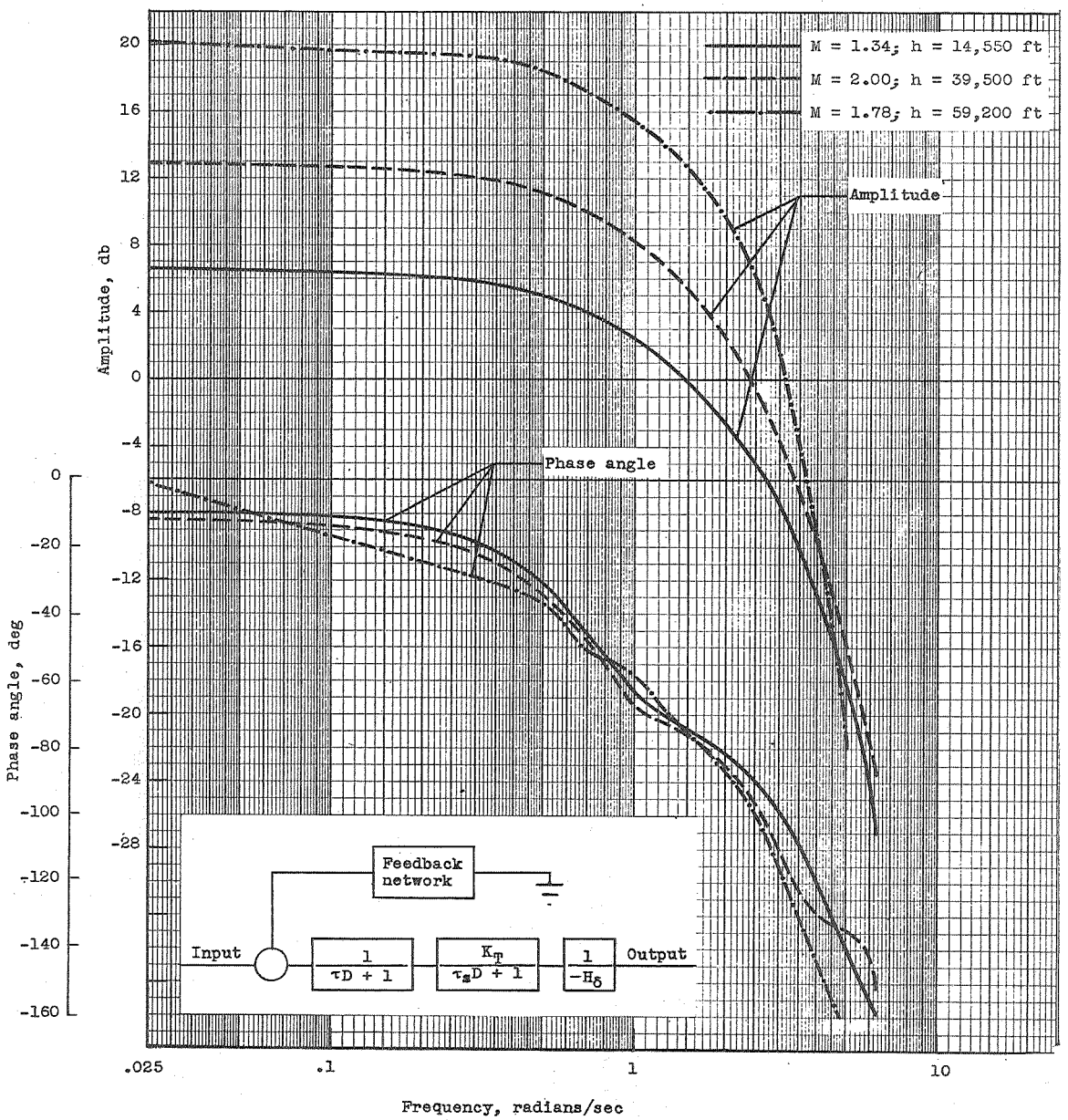

Figure 2.- Measured open-loop frequency response of torque-servo components, including lag network, under various spring loads simulating hinge moments due to control-surface deflections at three flight conditions.

CONFIDENTIAL

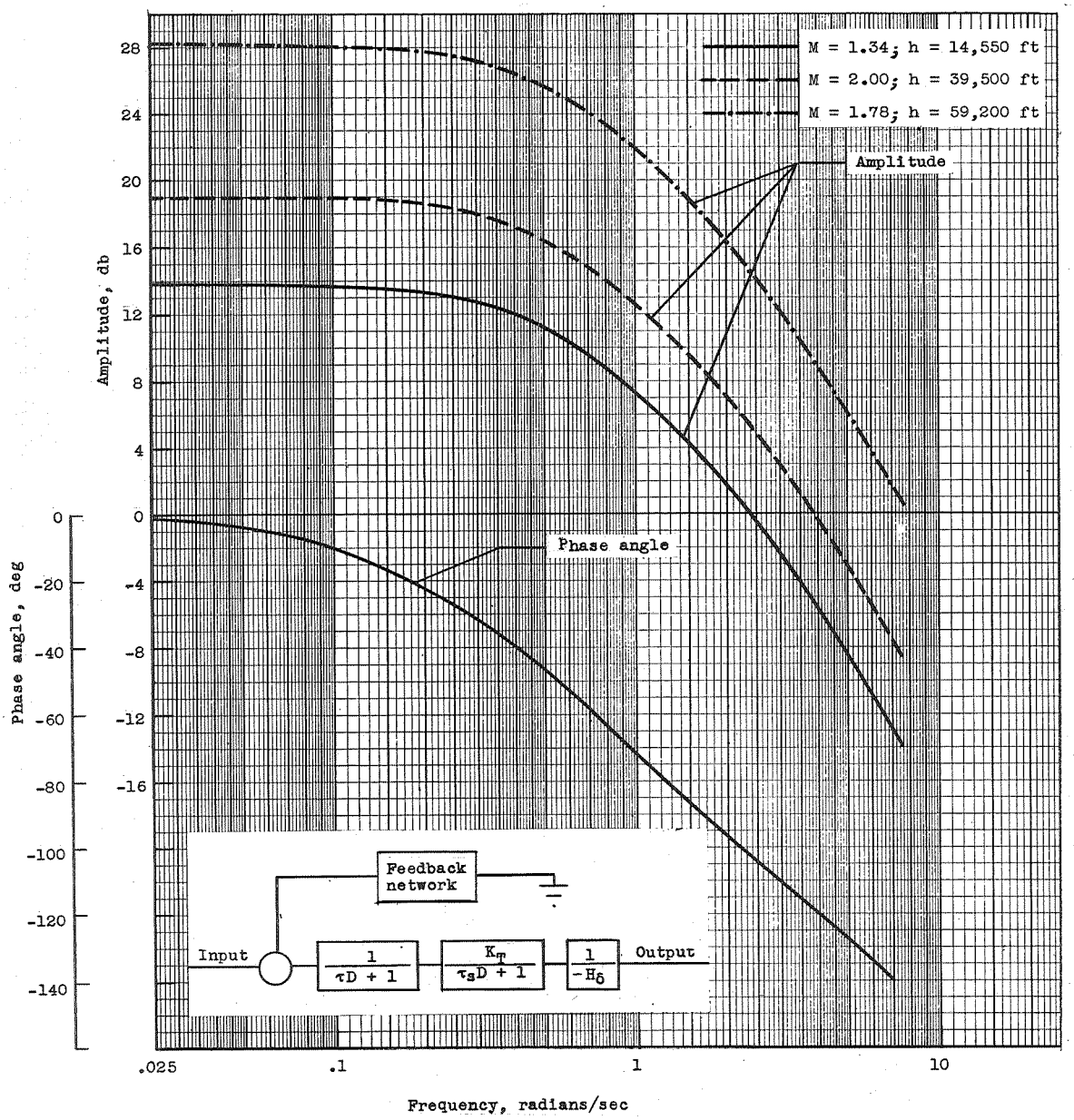

Figure 3.- Analytical open-loop frequency response of torque servo and lag network under hinge-moment loads due to control-surface deflection at three flight conditions.

I-456

CONFIDENTIAL

CONFIDENTIAL

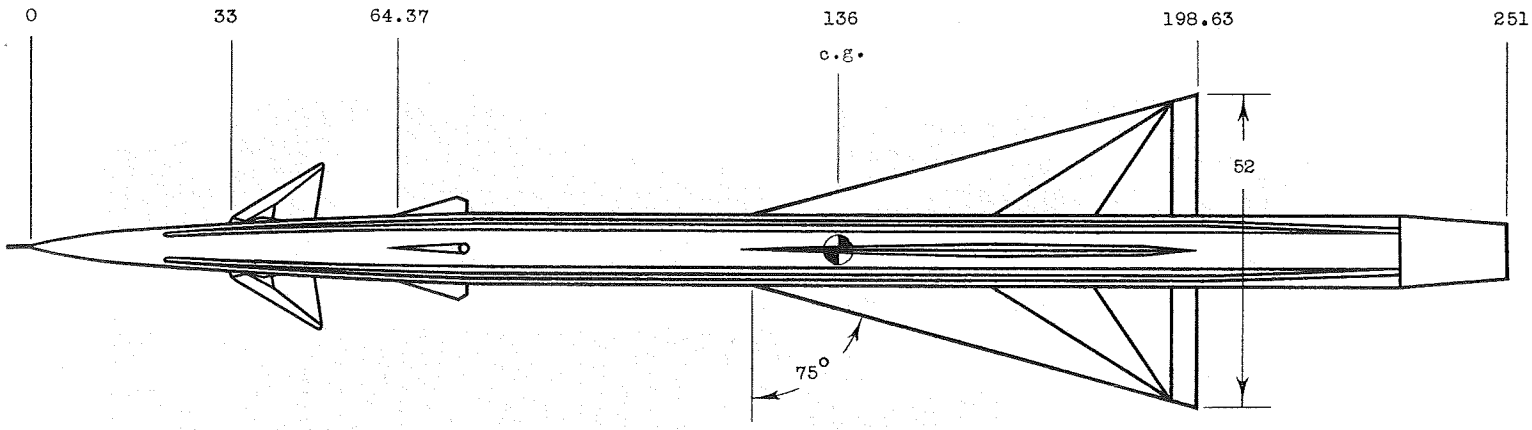

(a) Airframe.

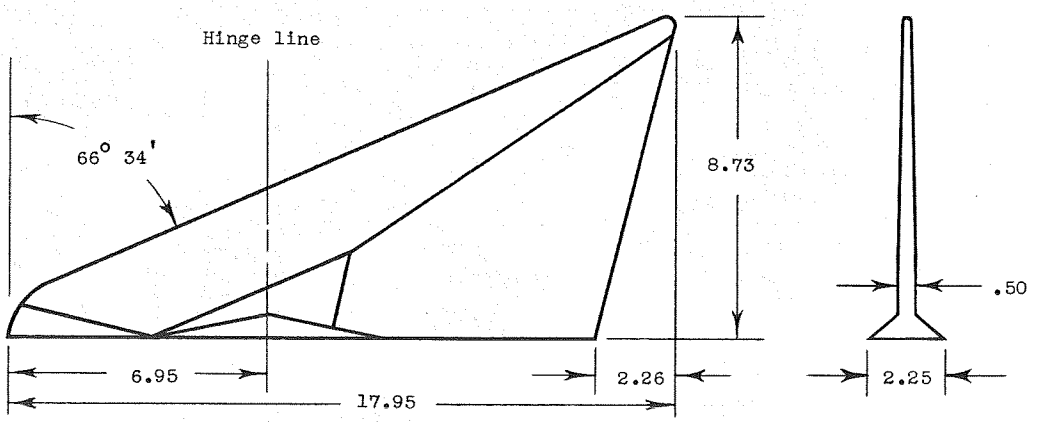

(b) Canard control surface.

Figure 4.- Sketch of flight-test-model configuration and control-surface plan form. All dimensions are in inches.

CONFIDENTIAL

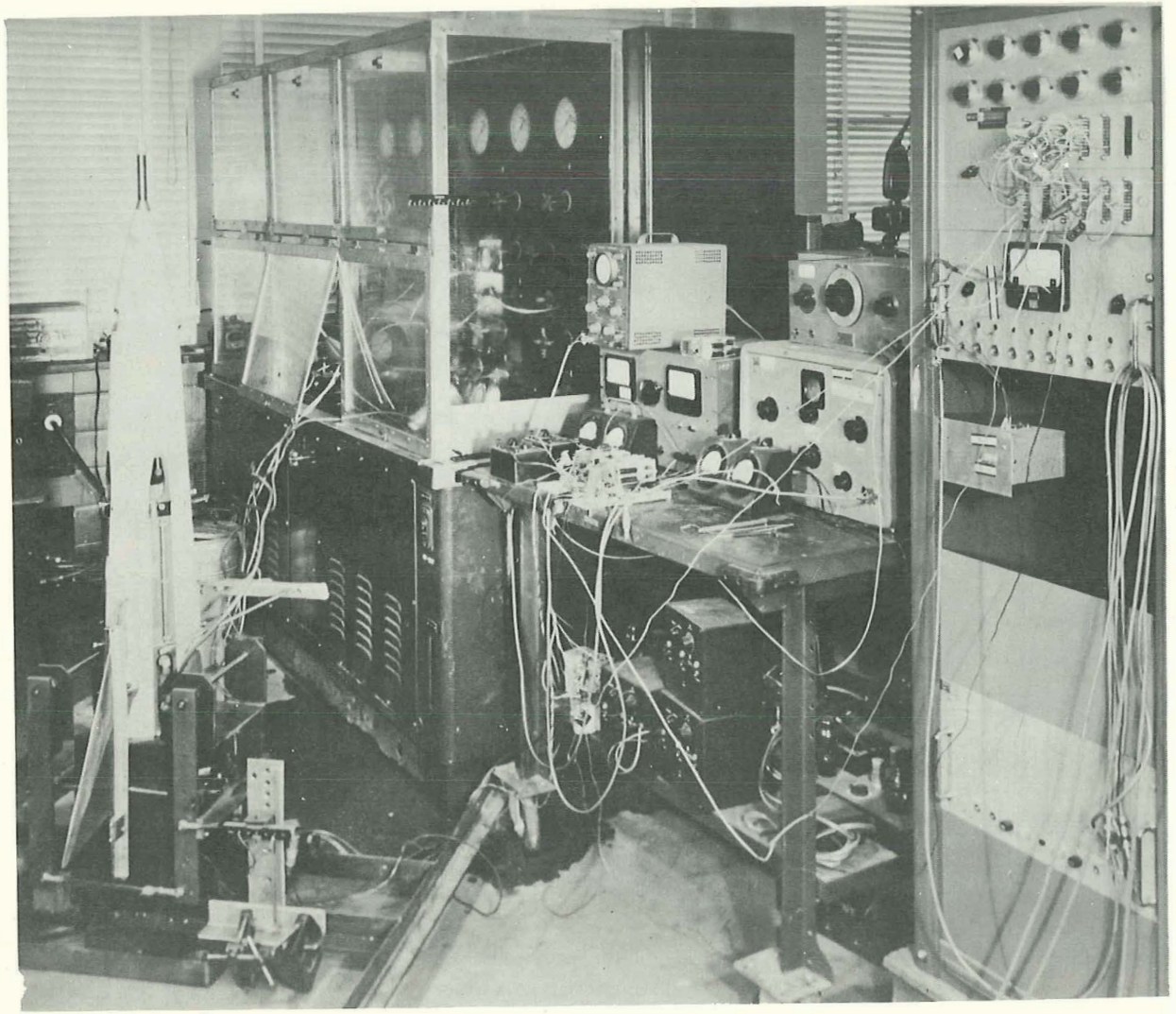

Figure 5.- Preflight simulator. L-58-236

CONFIDENTIAL

CONFIDENTIAL

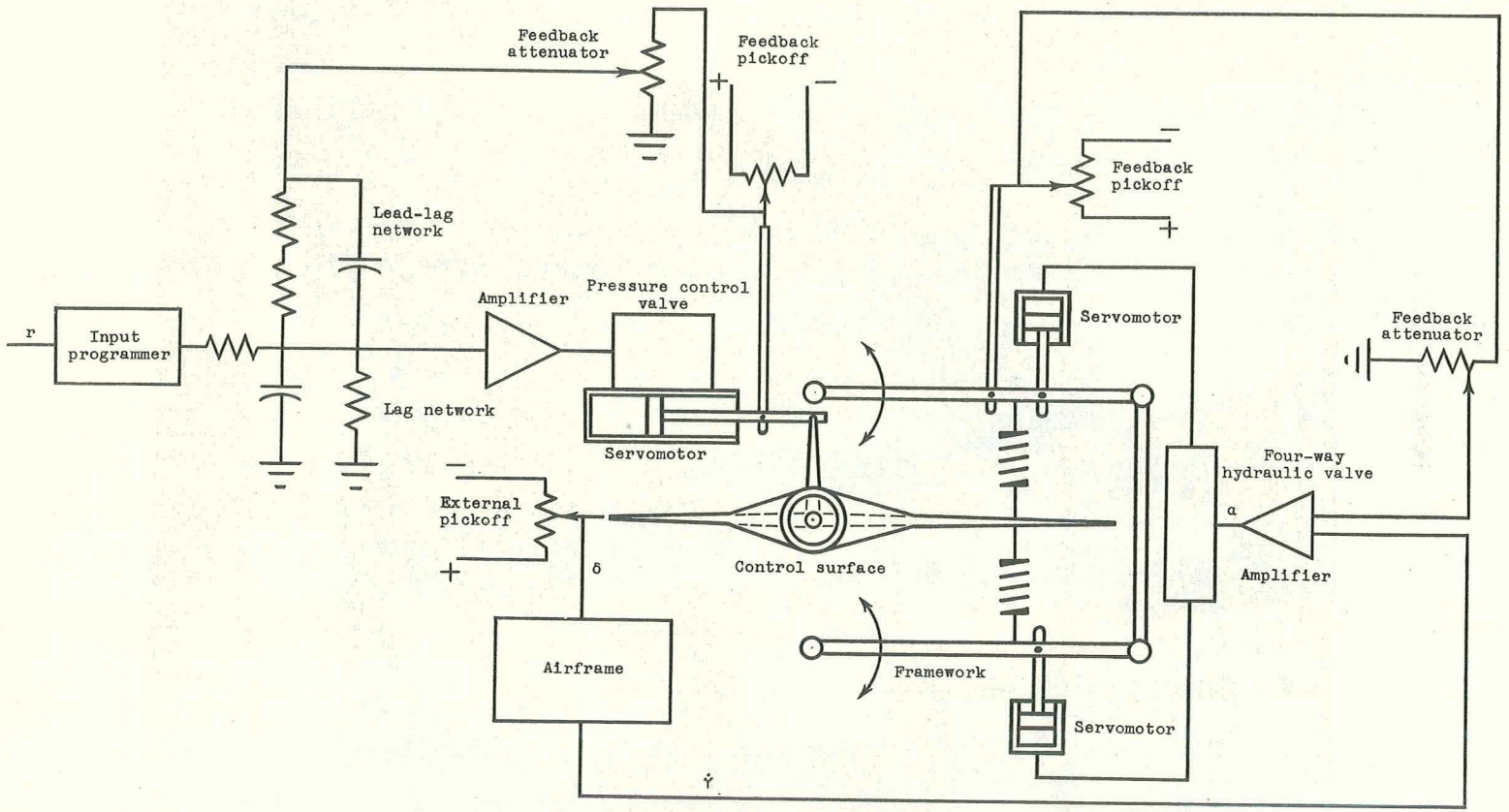

Figure 6.- Schematic diagram of preflight simulator and torque plus position servocontrol system.

CONFIDENTIAL

CONFIDENTIAL

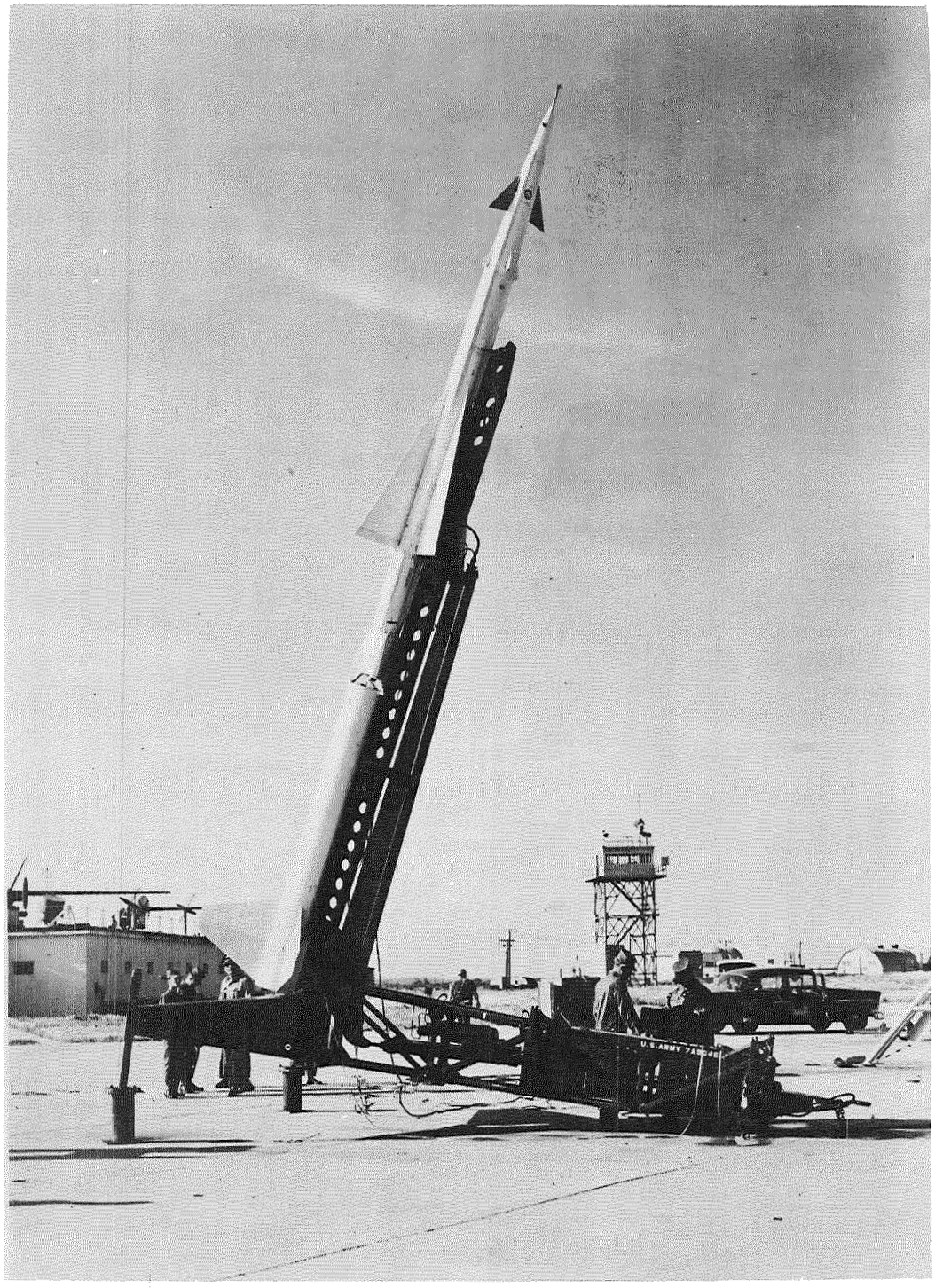

L-456

Figure 7.- Model and booster on launcher. L-58-2604

CONFIDENTIAL

L-456

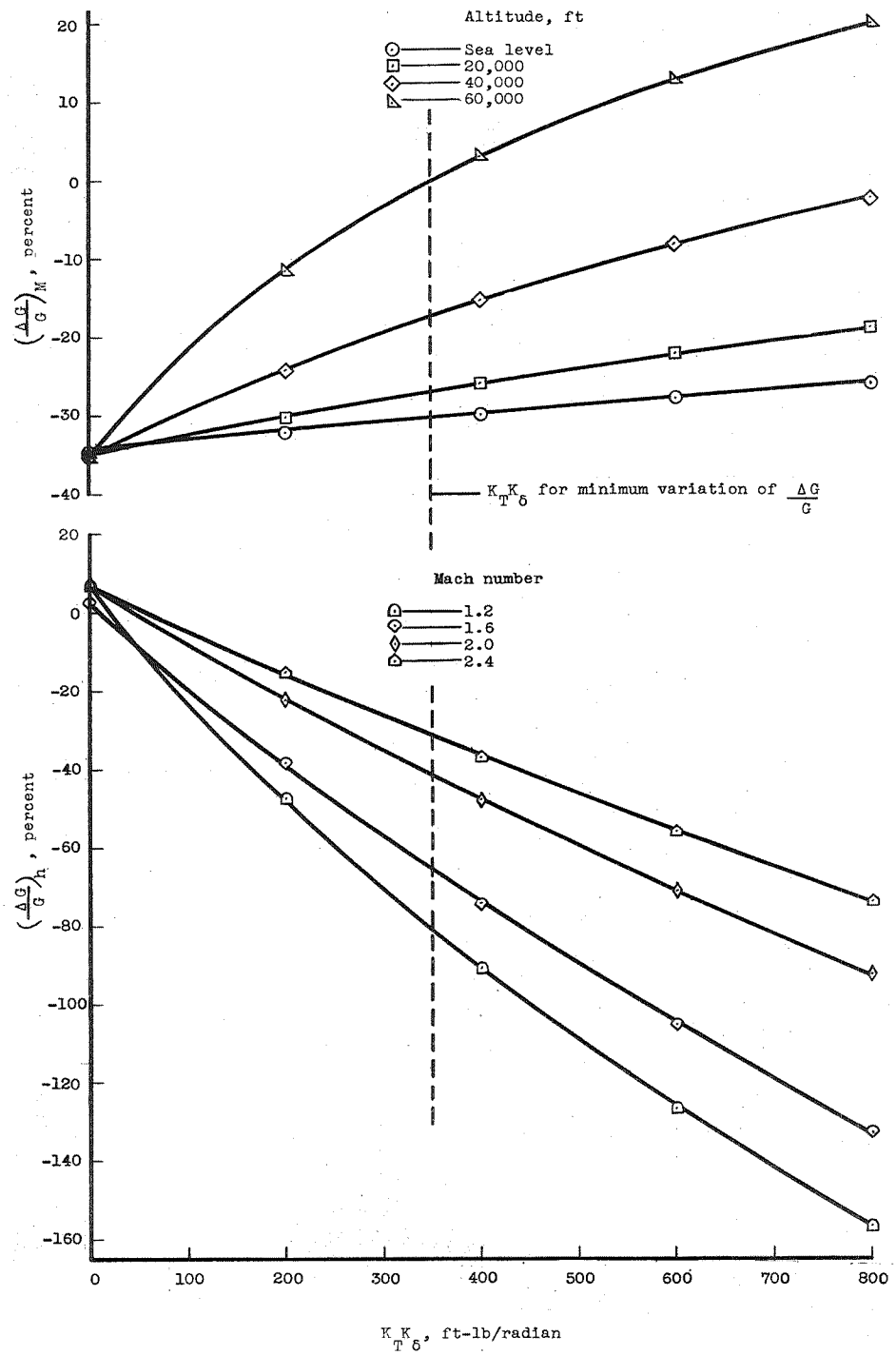

Figure 8.- Percentage variation of the static gain G of the torque plus position servo-actuated Nike-Ajax missile for an altitude change from sea level to 60,000 feet and Mach number change from 1.2 to 2.4.

CONFIDENTIAL

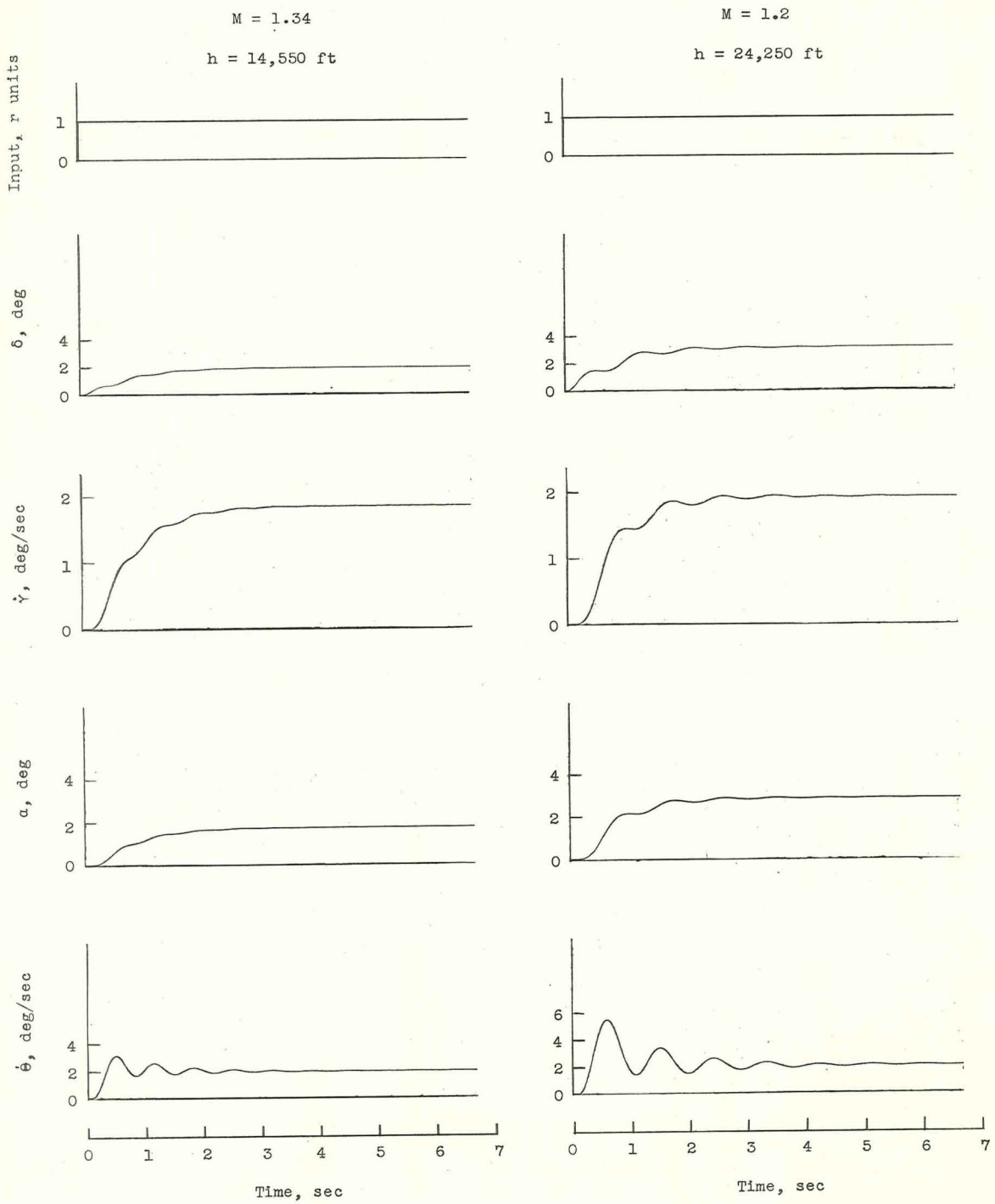

Figure 9.- Theoretical predicted responses to step input commands at four flight conditions based on preliminary analytical studies of the torque plus position servocontrol system in combination with the modified Nike-Ajax missile airframe.

CONFIDENTIAL

I-456

L-456

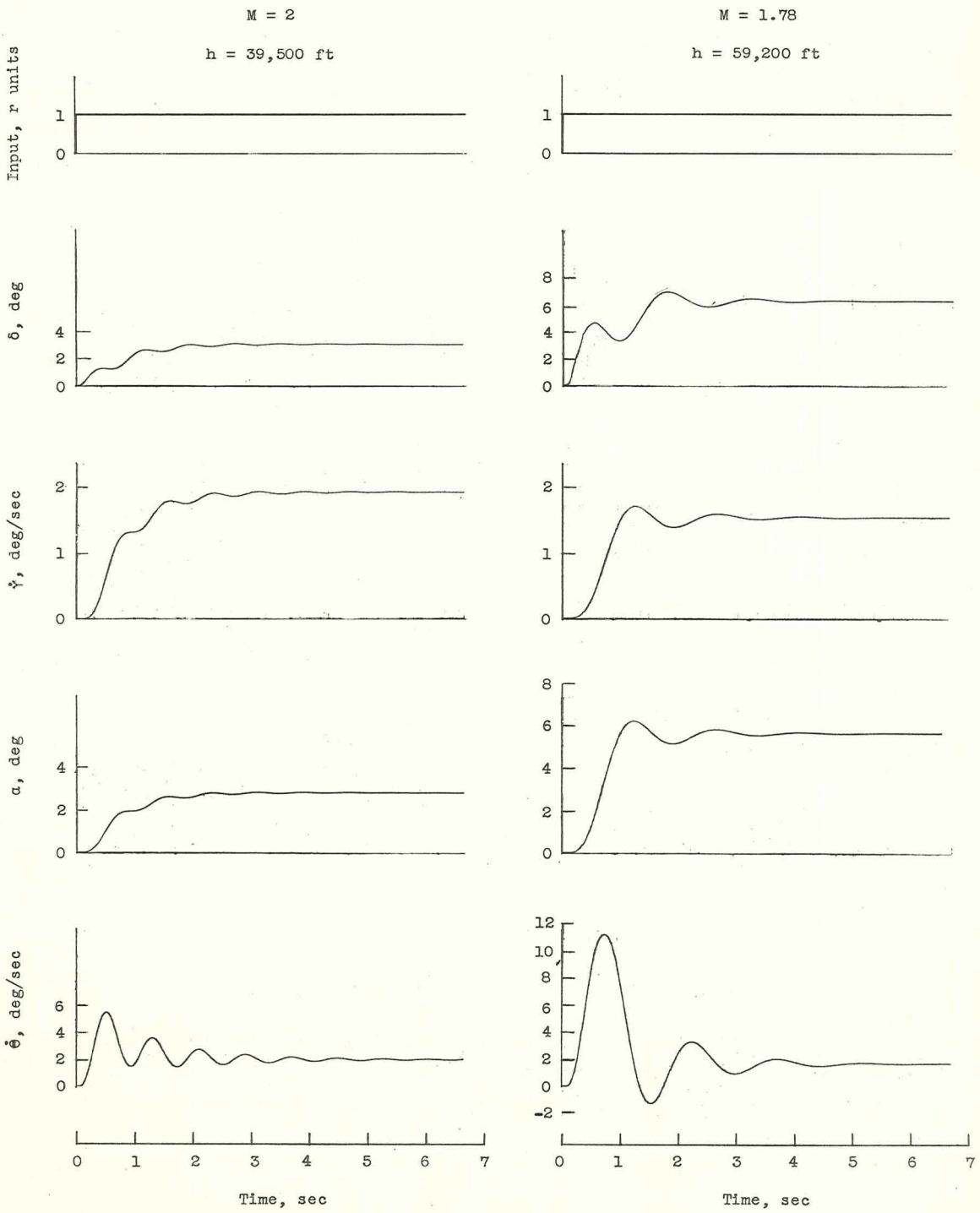

Figure 9.- Concluded.

CONFIDENTIAL

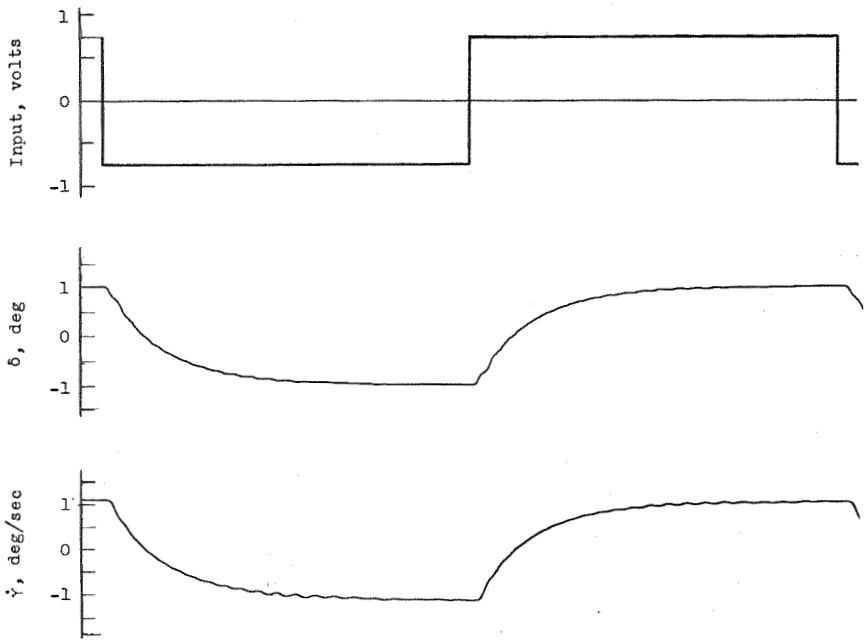

(a) M = 1.34; h = 14,550 feet.

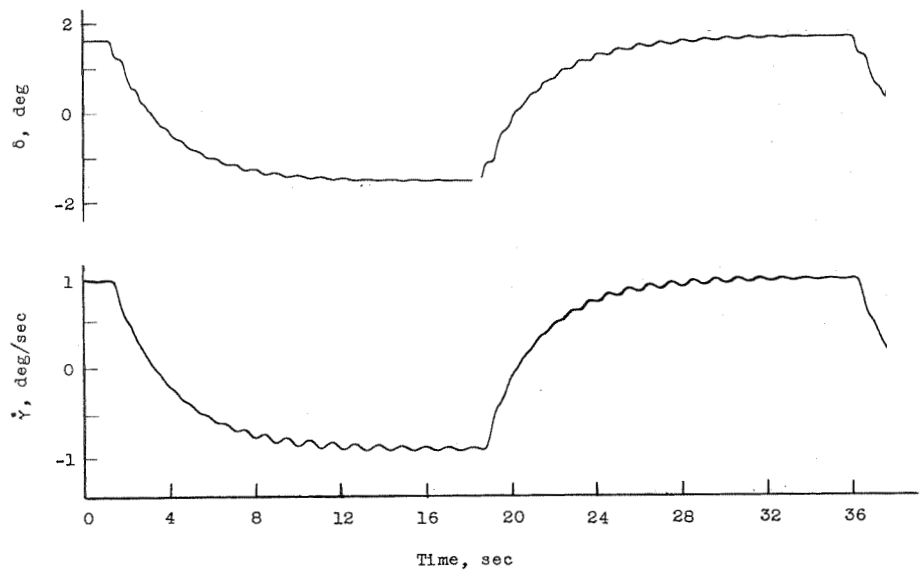

(b) M = 2.0; h = 39,500 feet.

Figure 10.- Preflight simulator responses of the torque plus position servocontrol system and simulated Nike-Ajax missile airframe at three flight conditions.

CONFIDENTIAL

CONFIDENTIAL

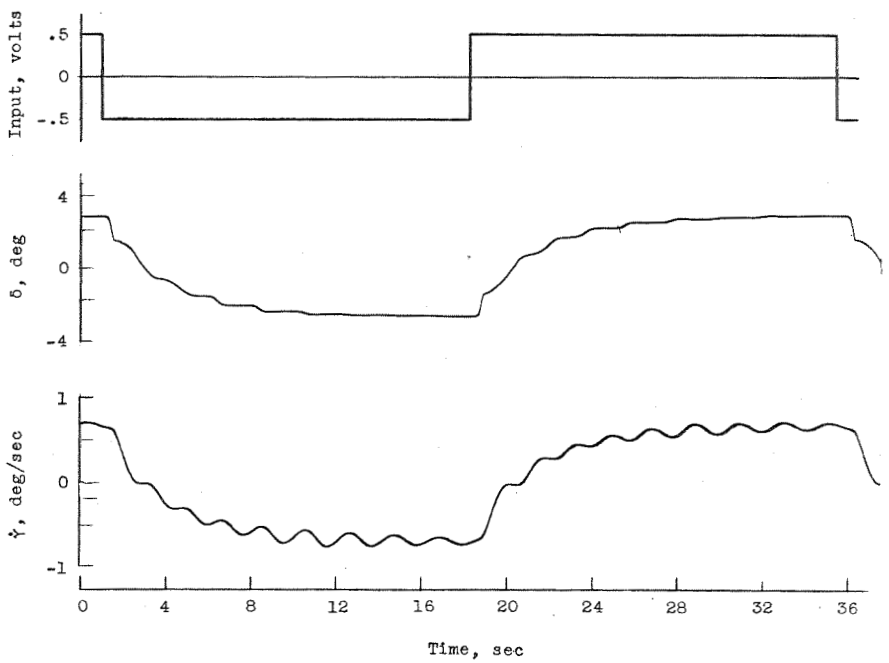

(c) M = 1.78; h = 59,200 feet.

Figure 10.- Concluded.

CONFIDENTIAL

CONFIDENTIAL

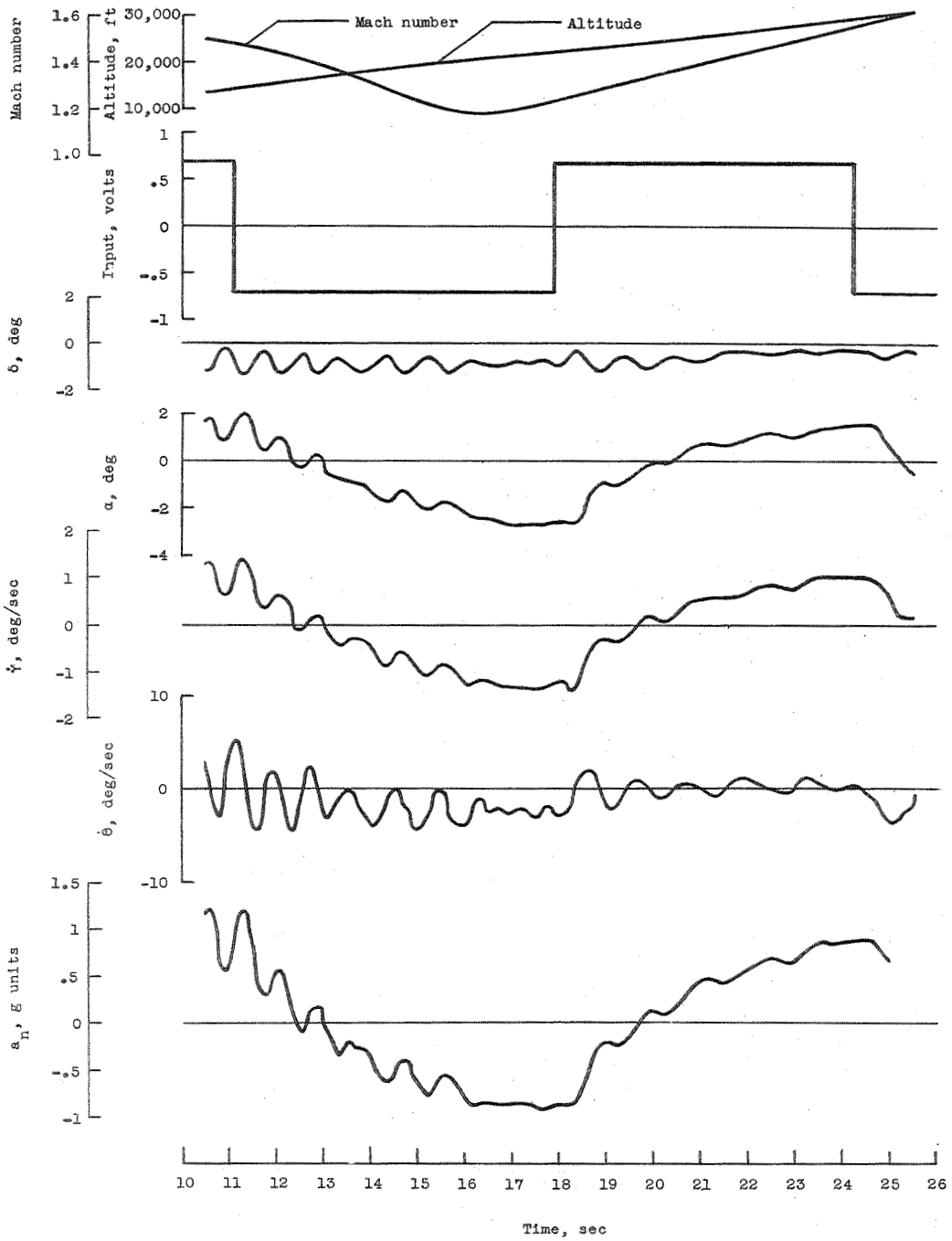

(a) δ, α, $\dot{\gamma}$, $\dot{\theta}$, and a_n from t = 10.5 to t = 25.5.

Figure 11.- Time histories of flight-test responses to command inputs obtained from telemeter records.

CONFIDENTIAL

I-456

L-456

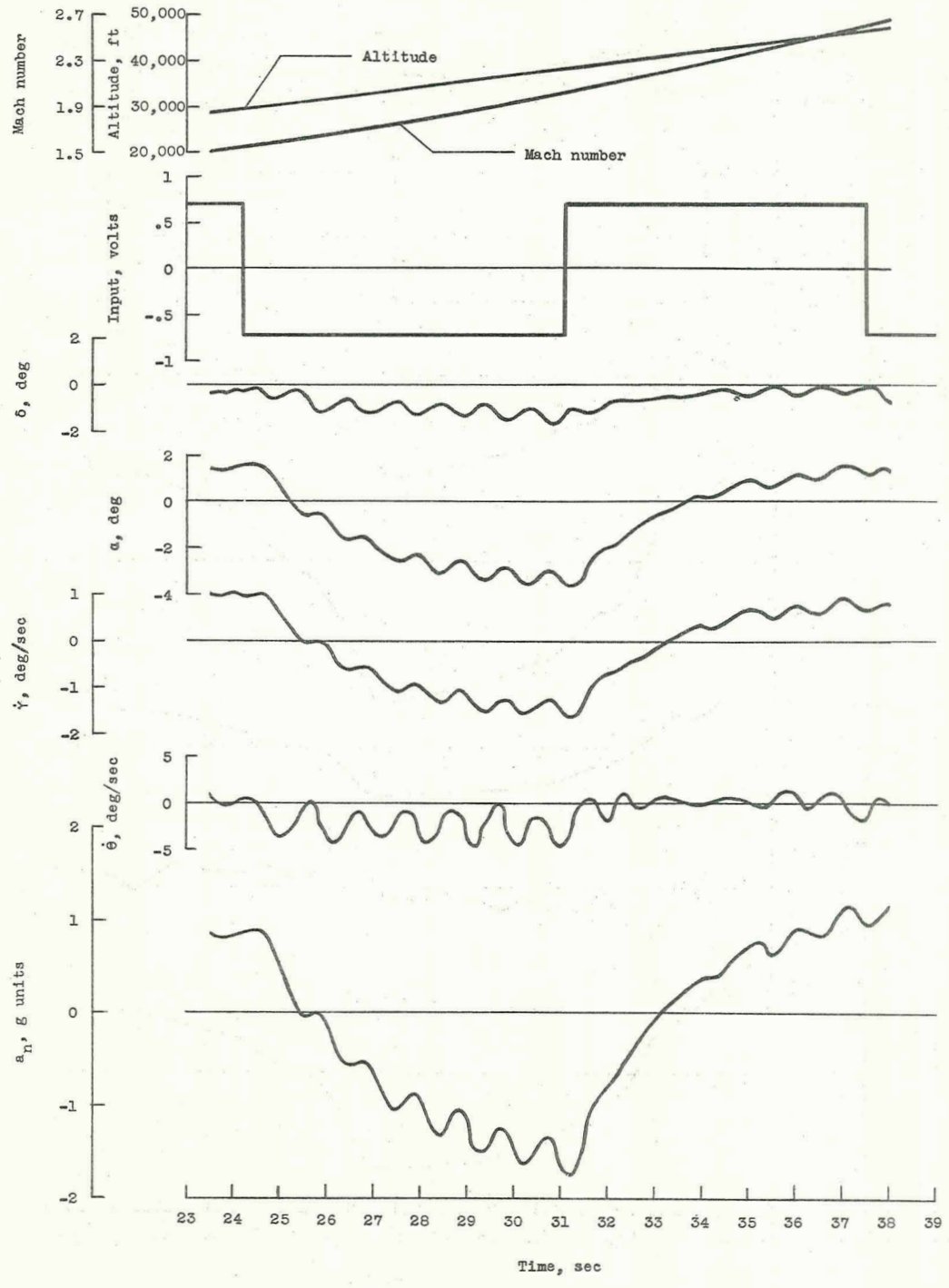

(b) δ, α, $\dot{\gamma}$, $\dot{\theta}$, and a_n from t = 23.5 to t = 38.

Figure 11.- Continued.

CONFIDENTIAL

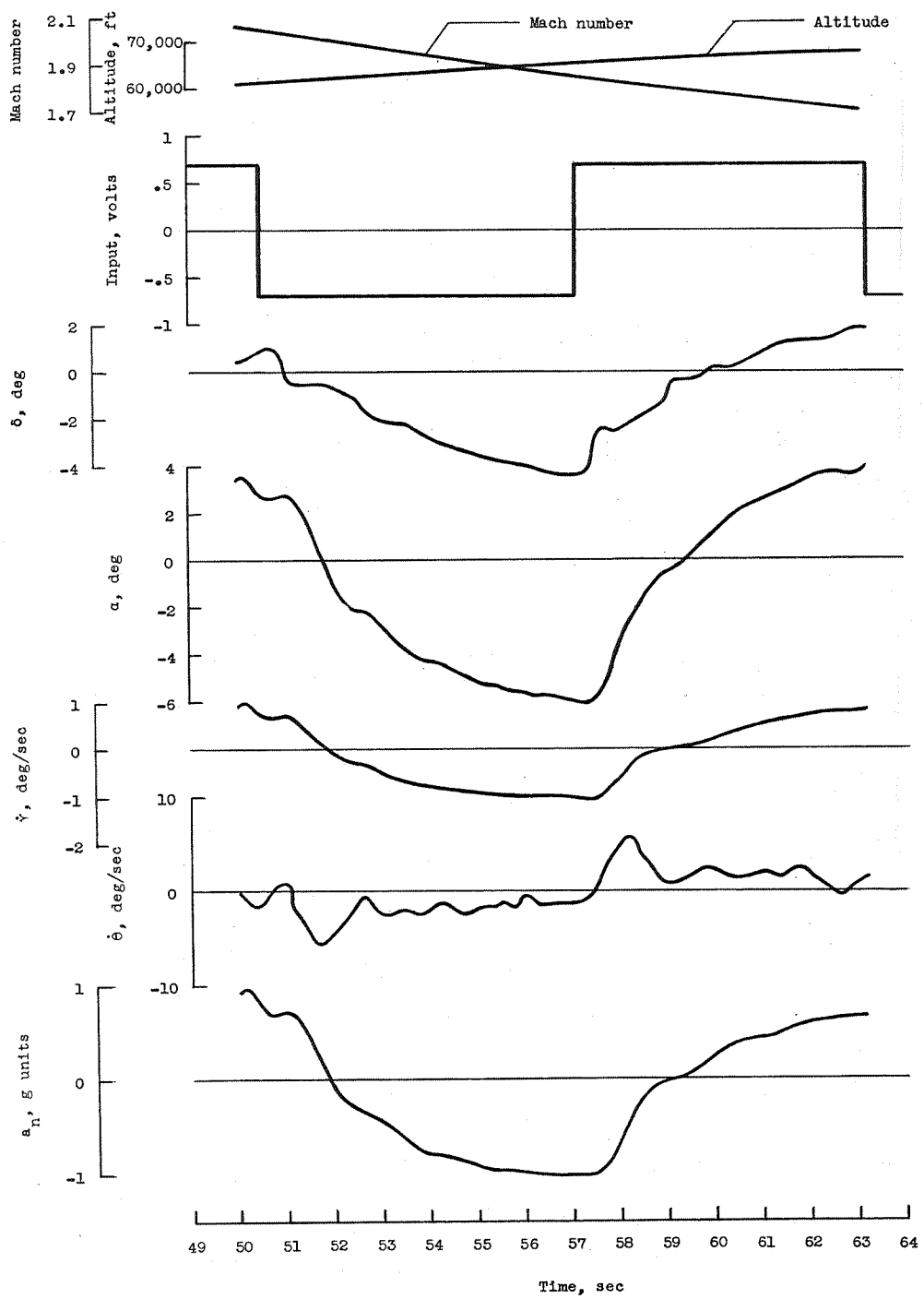

(c) δ, α, $\dot{\gamma}$, $\dot{\theta}$, and a_n from t = 50 to t = 63.2.

Figure 11.- Concluded.

CONFIDENTIAL

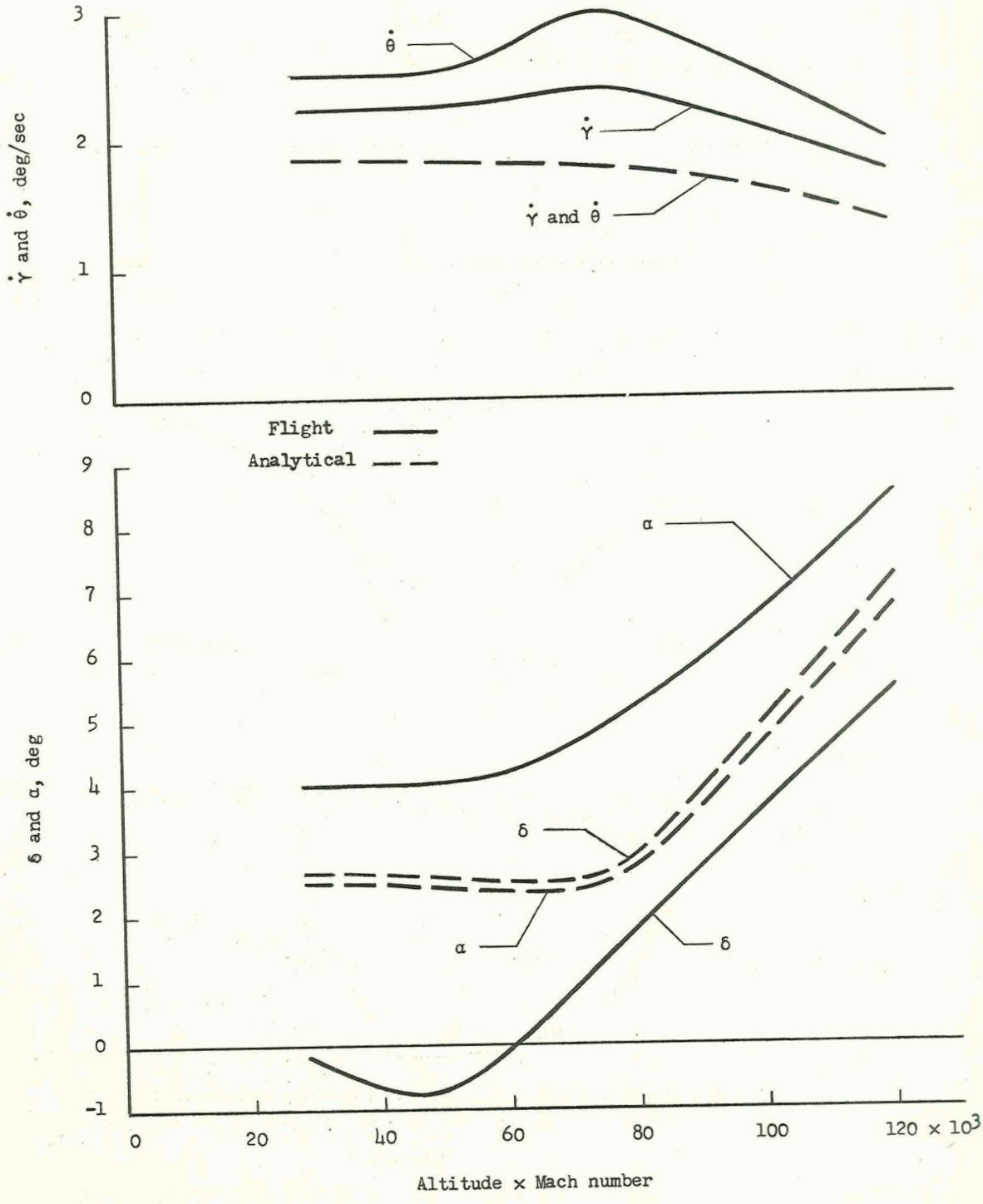

Figure 12.- Flight and analytical steady-state responses of δ, α, $\dot{\gamma}$, and $\dot{\theta}$.

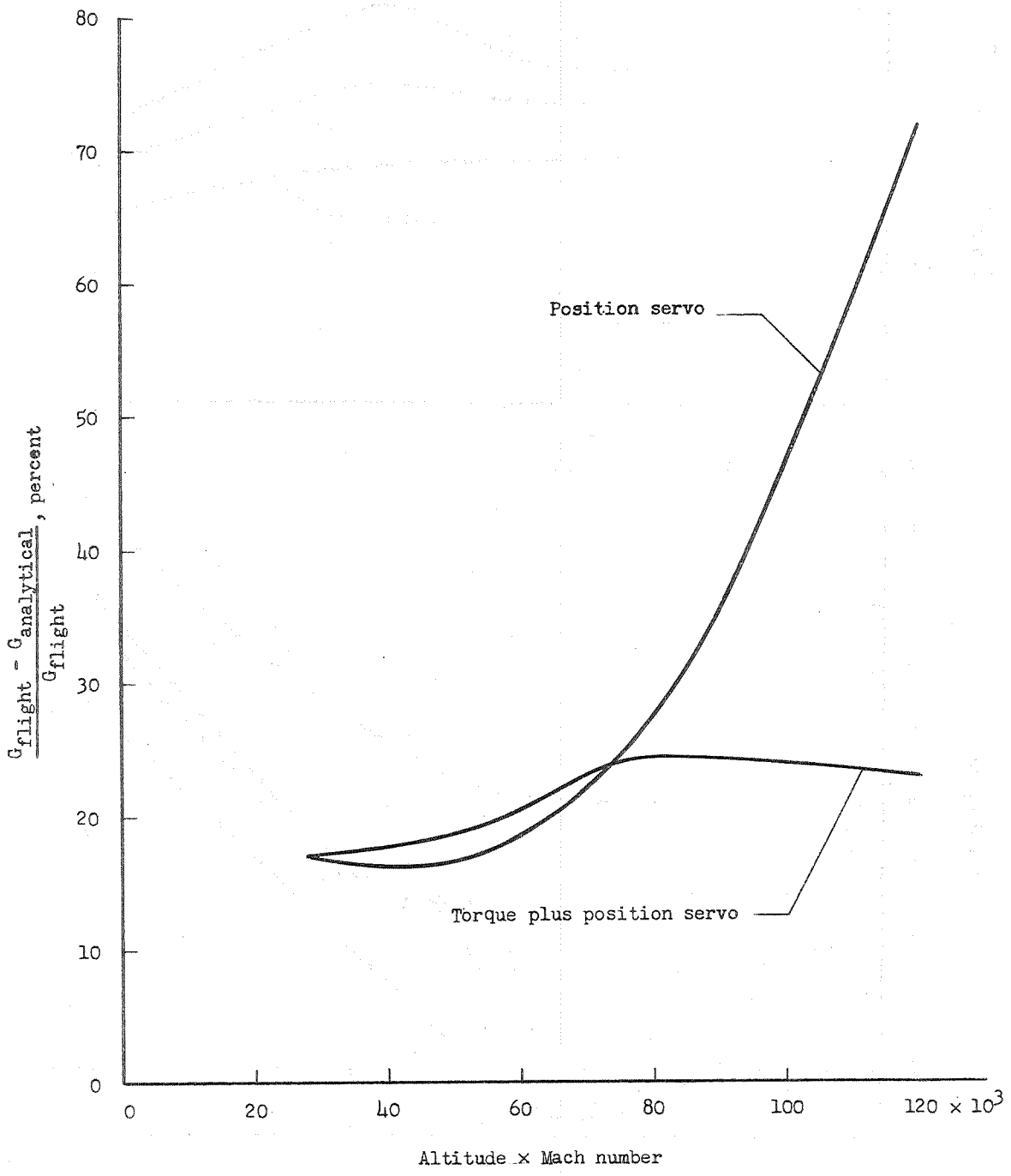

Figure 13.- Comparison of analytical steady-state responses of G obtained by using torque plus position and position servocontrol systems with flight results obtained by use of a torque plus position servo.

CONFIDENTIAL

I-456

L-456

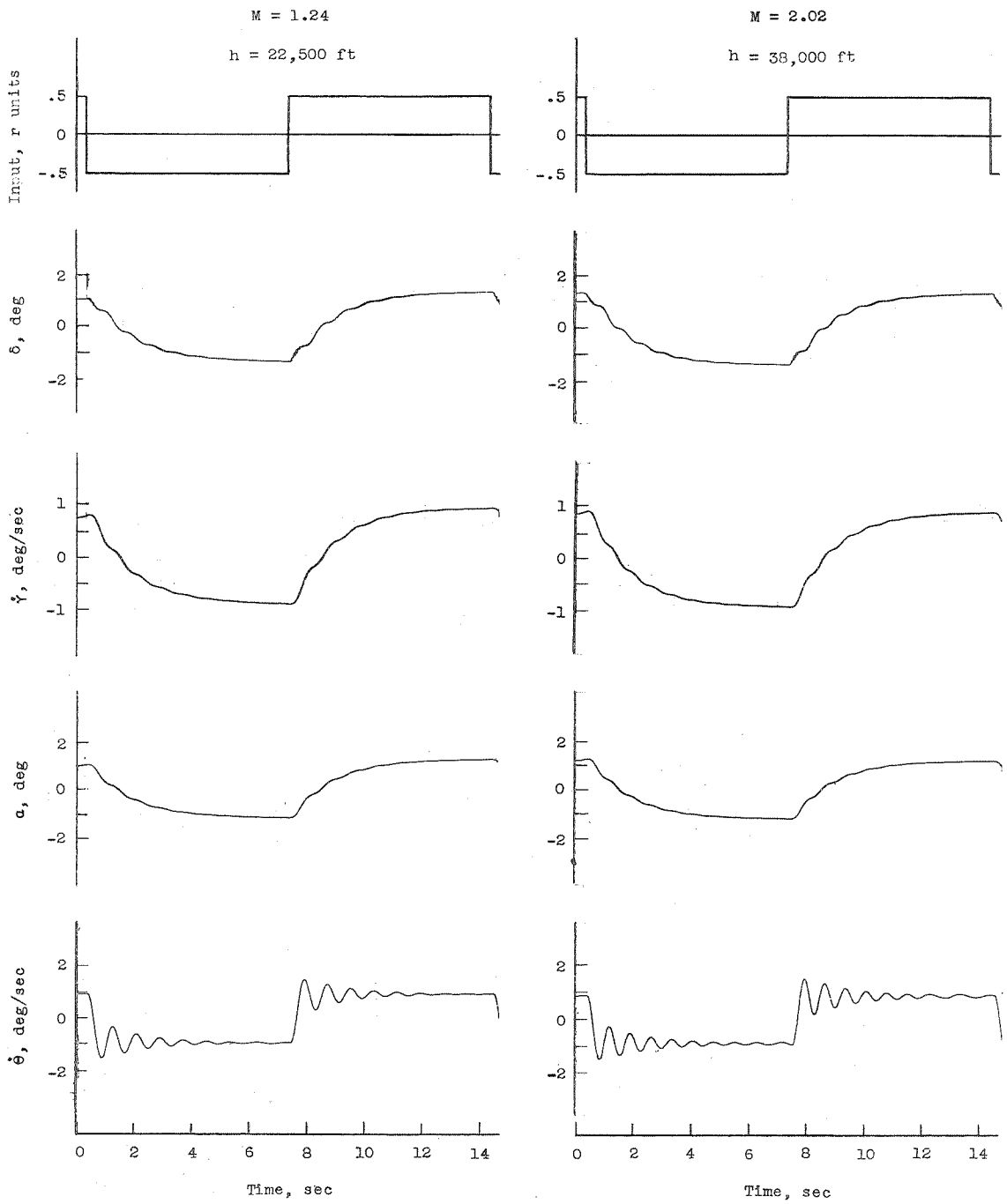

Figure 14.- Postflight simulated responses at three points along the actual flight-test trajectory using a linear representation of the control-system—airframe combination with coulomb friction substituted for control-surface viscous damping.

CONFIDENTIAL

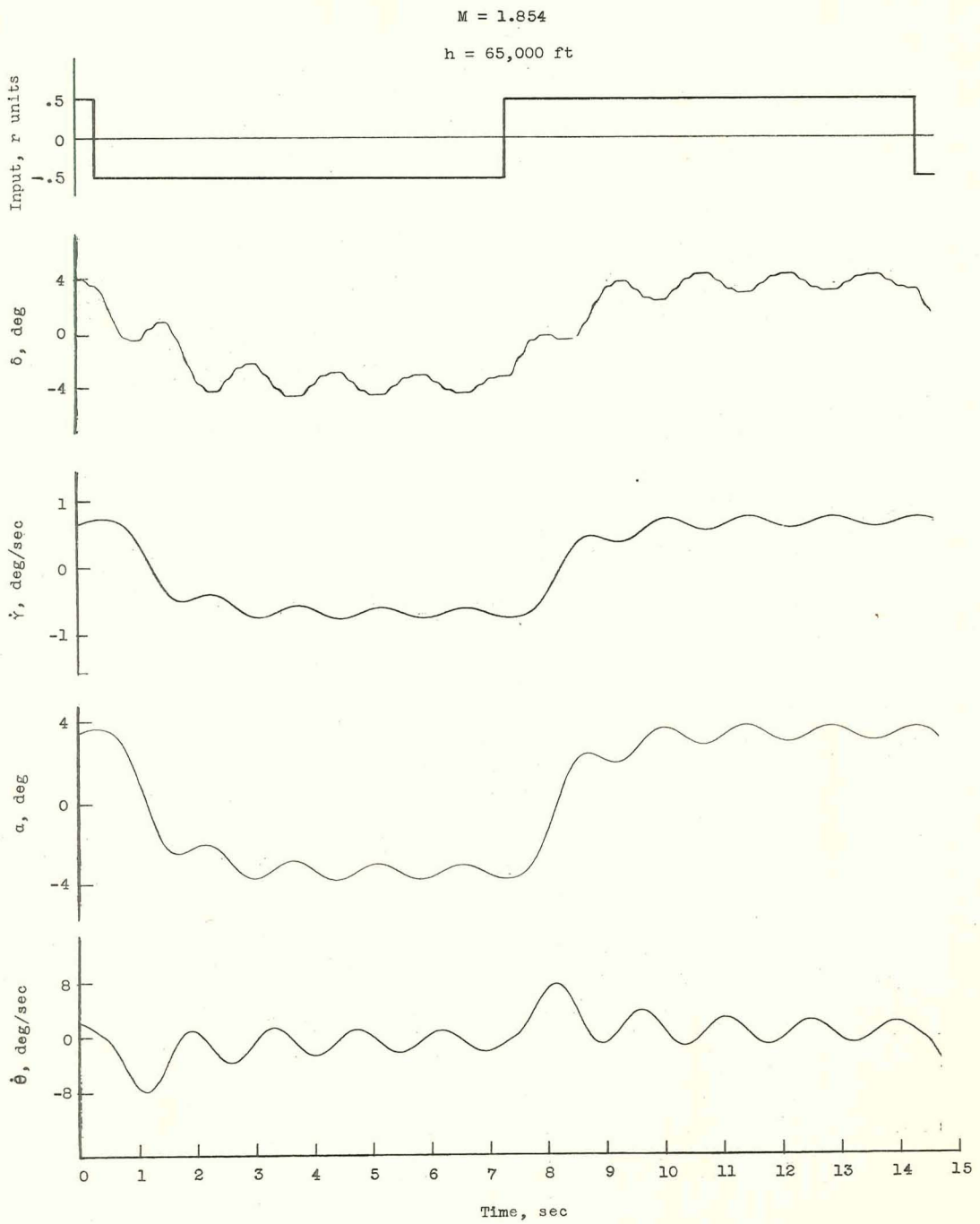

Figure 14.- Concluded.

CONFIDENTIAL

L-456

CONFIDENTIAL

CONFIDENTIAL